

Effect of Rectangular Cold-Formed Steel on the Behavior of Double-Skinned Profiled Steel Sheet In-Filled With Concrete under Axial Load

Salam Jasim Hilo, Wan Hamidon Wan Badaruzzaman, Siti Aminah Osman, and Ahmed W. Al Zand

Abstract---Finite element (FE) models are developed to investigate the axial load behavior of a composite wall that consists of a double-skinned profiled steel sheet (PSS) in-filled with normal concrete and strengthened with embedded rectangular cold-formed steel (CFS). In this study, axial load behavior is compared between the FE models and an existing experimental work, and highly accurate results are obtained. Seven FE models are established to study the effectiveness of three parametric studies, namely, various thicknesses of the PSS, embedded rectangular CFS without stiffener, and embedded rectangular CFS with stiffeners with two different shapes, to improve the axial load capacity of the composite wall system. The results of this study confirm that the ultimate axial load of the composite wall increased by approximately 3.3% when PSS thickness increased from 0.8 mm to 1.0mm. Moreover, adding two embedded rectangular CFS to the composite wall improves the ultimate axial load to approximately 24% and 34% when thickness is 0.8 mm and 1.0mm, respectively. Moreover, by adding stiffeners into the embedded rectangular CFS (0.8mm thick), the ultimate axial load of the composite wall is improved by up to 54% and 62% for L- and T-shaped stiffeners, respectively.

Keywords---Profiled steel sheet, double skinned, thin wall, composite wall, strengthening, cold-formed steel, stiffeners

I. INTRODUCTION

THE DSPSS in-filled with concrete is a type of composite wall that has been developed from composite flooring.

The advantages of this type of composite wall are convenient construction, timing, recyclability, and efficient behavior against axial loads [1]. However, during the construction stage, a PSS can function as a fixed formwork for infill concrete while simultaneously working as a bracing system for the structure frame against axial loads [2].

Salam Jasim Hilo, is with the Department of Civil and Structural Engineering, Universiti Kebangsaan Malaysia, Bangi, Selangor, Malaysia. On leave from University of technology, Baghdad, Iraq (corresponding author's phone: +60147247453; e-mail: eng.salamjh@gmail.com).

Wan Hamidon Wan Badaruzzaman, Department of Civil and Structural Engineering, Universiti Kebangsaan Malaysia, Bangi, Selangor, Malaysia. (Co-author's phone: +60193105697; e-mail: wanhamidon@gmail.com).

Siti Aminah Osman Department of Civil and Structural Engineering, Universiti Kebangsaan Malaysia, Bangi, Selangor, Malaysia. (Co-author's phone: +60196310129; e-mail: saminah@eng.ukm.my).

Ahmed W. Al Zand Department of Civil and Structural Engineering, Universiti Kebangsaan Malaysia, Bangi, Selangor, Malaysia. Co-author's phone: +601128147460; e-mail: ahmedzand70@gmail.com).

Numerous studies have examined the behavior of composite walls under the effects of exerting different load types [1-5], providing openings [6-10], enhancing wall strength by using high-strength infill concrete [11, 12], and enhancing the interaction between a PSS and its core concrete [4, 12, 13]. In addition, the strengthening of composite walls by adding steel wires and bolts was studied in [12], whereas strengthening by adding a pair of steel frames connected by bolts was researched in [4]. The failure mode was governed by the vertical splitting and crushing of concrete in the mid-portion, followed by the overall bulging of the steel sheet in [12]. Meanwhile, the failure mode was attributed to the diagonal concrete cracking and buckling of both PSSs in [4].

In the present study, nonlinear FE analysis was developed to investigate the behavior and axial load capacity of a composite wall system. The models were then compared with an existing experimental work conducted by Wright (1998) to verify the validity of the FE models. In addition, three parametric studies were suggested to improve the axial load capacity of the wall. These parameters included using varying PSS thicknesses and providing embedded rectangular cold-formed steel (CFS) both with and without stiffener.

II. FINITE ELEMENT MODEL SIMULATION

The FE models were established based on a version similar to that of the composite experimental wall in [1]. several models were generated to investigate the axial load behavior of the composite wall system by using the FE software Abaqus/CAE [18]. The FE models generally consisted of double-skinned PSS in-filled with normal concrete for the control model, whereas the other models were constructed by using the same wall system with embedded rectangular CFS with and without internal stiffeners designed with different shapes.

A. Modeling wall assembly and boundary conditions

The FE models were generally generated from seven parts. These parts included two PSSs (on both sides of wall), a core concrete, two embedded rectangular CFS, and two steel supports plates (top and bottom), as shown in Fig. 1. Two types of elements were selected to model the core concrete: the linear hexahedral element (C3D8R) for the main core concrete elements and the linear triangular prism (C3D6) for the corner elements. The former elements were also adopted for the steel support plates. Meanwhile, the linear quadrilateral shell element (S4R) was adopted for the PSS and the embedded rectangular CFS.

A tie constraint option was assigned to represent the surface interaction between the support plates and the other wall parts at the top and bottom of the composite wall system. Meanwhile, tangential behavior with a penalty friction coefficient equal to 0.5 was assigned to the surface interaction between the PSS and the core concrete, as well as between the embedded rectangular CFS and the same core concrete.

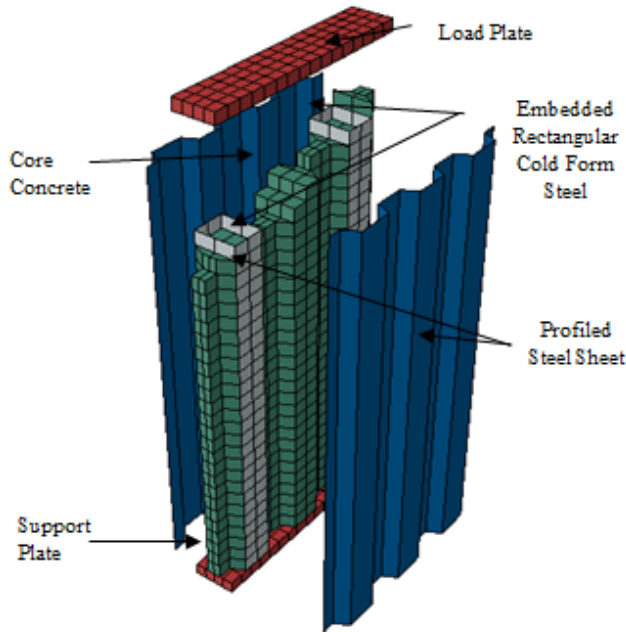


Fig 1. Main parts of the FE composite wall system

Furthermore, to eliminate out-of-plane displacement, a steel plate was provided at the bottom of the FE models to represent the fixed support plate; meanwhile, another plate was provided at the top of the models to represent the loading plate. In addition, the displacement of the three degrees of freedom at the bottom face of the support plate was restrained to implement the fixed support system along the x, y, and z directions. Meanwhile, the top plate was restrained with the top surface elements along the horizontal direction (x and z) while releasing the vertical direction (y) to represent the loading movement along this direction and the real loading scenario.

B. Core concrete material

For the core concrete, a compressive stress-strain relationship (shown in Fig. 2a) was adopted to simulate concrete behavior during compression [14-16]. Both the compressive concrete stress value (f_c) and concrete strain function (ϵ_c) can be derived from the following equation:

$$\frac{f_c}{f'_c} = \frac{n(\epsilon_c/\epsilon_o)}{n-1+(\epsilon_c/\epsilon_o)^{nK}} \tag{1}$$

where f'_c is the ultimate compressive strength of the concrete; n is a curve-fitting factor, which can be considered as $n = 0.8 + \frac{f'_c}{17}$ or $n = \frac{E_c}{E_c - E'_{t_c}}$; E_c is the initial tangent modulus, which can be obtained from the formula, $E_c = 6900 + 3300\sqrt{f'_c}$; ϵ_o is the strain when f_c reaches f'_c , and can be taken as $\epsilon_o = \frac{f'_c}{E_c} \left(\frac{n}{n-1} \right)$; and E'_{t_c} is the tangent modulus of concrete at f'_c that can be calculated as follows:

$E'_{t_c} = f'_c/\epsilon_o$. Finally, the factor that controls the slope of

the stress-strain curve is K , which can be obtained through the following conditions:

If $(\epsilon_c/\epsilon_o) \leq 1$, then $K = 1.0$;

Whereas if $(\epsilon_c/\epsilon_o) > 1$, then $K = 0.67 + \frac{f'_c}{62} \geq 1.0$.

Concrete damage plasticity option, which is available in the FE software Abaqus, was used to identify the plastic, elasticity, compressive, and tensile properties of the concrete material. The concrete compressive strength used in this study is 29.2MPa, which is the same value adopted in [17].

C. PSS and embedded rectangular CFS

The obtained properties of the CFS (the PSS and the embedded rectangular section) were the same as those of the materials in the existing experimental test [1], which are given in TABLE I. Whilst, the details and dimensions of PSS are presented in TABLE II along with the details of the PSS. In the mechanical list of the material section in Abacus/CAE, the elastic and plastic values were obtained to identify the properties of the CFS. However, the true stress (σ_{true}) and the logarithmic plastic strain (ϵ_{ln}^{pl}) can be derived from the following equations:

$$\sigma_{true} = \sigma_{nom}(1 + \epsilon_{nom}) \tag{2}$$

$$\epsilon_{ln}^{pl} = \ln(1 + \epsilon_{nom}) - \frac{\sigma_{true}}{E} \tag{3}$$

Meanwhile, the CFS stress-strain relationship is presented in Fig. 2b.

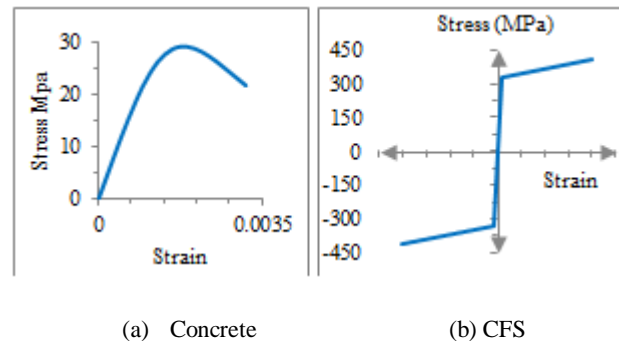


Fig 2. Stress-strain relationship for concrete and CFS material

TABLE I
PROPERTIES OF THE CFS (ALL UNITS ARE IN MPA=N/MM²)
(WRIGHT, 1998)

| Yielding strength | Ultimate strength | E value |
|-------------------|-------------------|---------|
| 329 | 411 | 186,000 |

TABLE II
DETAILS OF THE PSS USED IN THE TEST (WRIGHT, 1998)

| Profiled Steel Sheet name | Profiled Steel Sheet Geometry | p | d | f1 | f2 | w | t |
|---------------------------|-------------------------------|-----|----|-----|-----|----|-----|
| ward multideck 60 | | 323 | 60 | 119 | 142 | 31 | 0.9 |

III. FINITE ELEMENT DISCRETIZATION

In order to obtain an accurate FE result, a suitable meshing with convergence studies were conducted on the composite wall system. Six FE models with varying mesh sizes were selected to identify the best models used in this study. The ultimate axial load with number of elements relationship, which considered various mesh sizes of the FE models, is presented in Fig. 3. As shown clearly in the figure, the FE models with 7744 and 13455 elements presented ultimate axial loads with significantly close values, which were 2221 kN and 2226 kN, respectively. Therefore, the FE model with 7744 elements was selected to represent the general FE models (will name as the Control morel for all following comparisons in this study) in this study given that this model provides adequate axial load value and optimum time to run the models in normal computers.

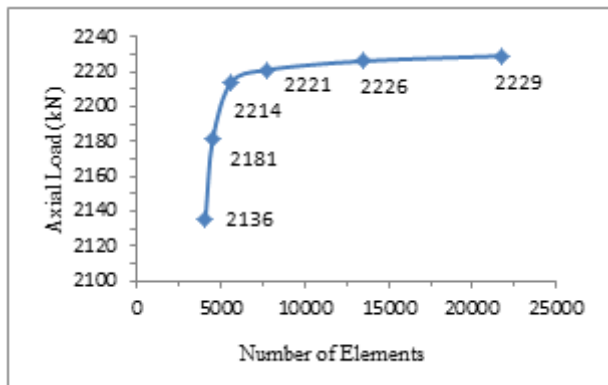


Fig 3. Convergence study of the FE models

IV. VALIDATING THE FE SIMULATION MODELS

The accuracy of the suggested FE models was verified by comparing them with the results in the experimental work conducted by [1]. However, this previous work was carried out in three tests, during which the investigated materials were subjected to a predominantly axial load regime to independently investigate the ultimate capacities of the composite wall system, the PSS, and the core concrete. The composite wall system generally consisted of the DSPSS called Ward Multideck 60 in-filled with normal concrete (with the same material properties explained in Section (2.2, 2.3). Furthermore, to increase the interaction between the concrete and the PSS, tied hook connectors were used as shown in Fig. 4. Model 9 from the experimental work was selected to verify the present study. This model has a total wall height of 1800 mm, an assembly thickness of 180 mm, and PSS thickness of 0.9mm.

A highly accurate comparison was obtained between the results of present FE analysis and those of the experimental work, as shown in TABLE III and Fig. 5.

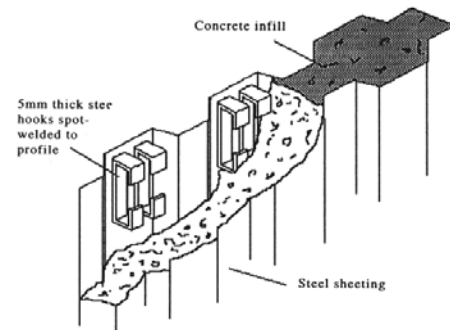


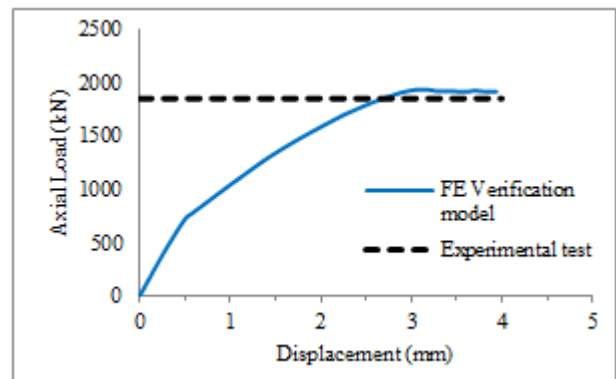
Fig 4. Main components of composite wall test number (Wright, 1998)

Fig 5.

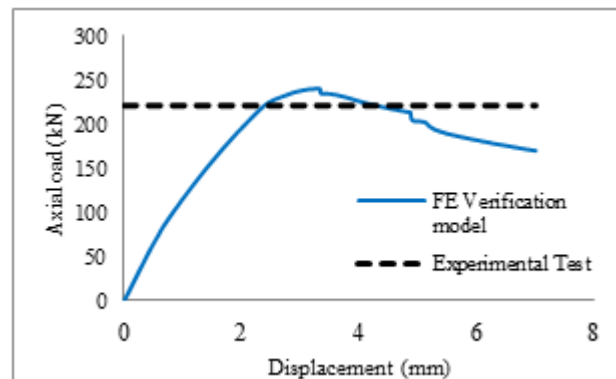
TABLE III

COMPARISON OF THE ULTIMATE AXIAL LOAD BETWEEN THE PRESENT STUDY AND THE EXPERIMENTAL TEST

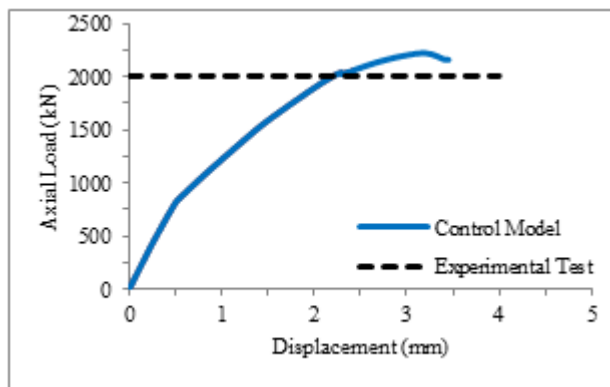
| Models | Experimental test [1] (kN) | FE Models (kN) | Deviation from the experimental value (%) |
|----------------|----------------------------|----------------|---|
| Core concrete | 1848 | 1933 | +4.5 |
| PSS | 221 | 240 | +8.5 |
| Composite wall | 2007 | 2221 | +10.6 |



a- Core Concrete Only



b- PSS Only



c- Composite wall system

Fig 6. Axial load–displacement curves of the present FE analysis and the experimental test

V. PARAMETRIC STUDIES

Based on the accepted comparisons with the existing experimental work, three parametric studies were suggested for further analysis etc., the effectiveness of various thicknesses of PSS, employing embedded rectangular CFS with and without internal stiffeners on the behavior of the composite wall system.

A. Effect of PSS thickness

Two FE models with different PSS thicknesses (0.8 mm and 1.0 mm), named PSS1 and PSS2, were adopted to explore the behavior of the composite wall system. As shown in TABLE VI and Fig. 6, the thicknesses exhibited no significant effect on the ultimate load and behavior of the composite wall. Model PSS1 demonstrated a reduction in the ultimate axial load of–1.5% when the thickness was 0.8 mm compared with the control model (model used to verify the study), which had a thickness of 0.9 mm. Meanwhile, model PSS2 presented an increase in the ultimate axial load of +1.8% when the PSS with 1.0 mm thickness was used. Therefore, for economical purposes, PSS with 0.8 mm thick was suggested.

TABLE IV
AXIAL LOAD RESISTANCE OF THE COMPOSITE WALL THAT IS ATTRIBUTED TO PSS THICKNESS

| Models | Profiled Steel Sheet Thickness (mm) | Axial Load Resistance (KN) | Displacement (mm) | Deference Percentage |
|---------------|-------------------------------------|----------------------------|-------------------|----------------------|
| Control Model | 0.9 | 2221 | 2.70 | - |
| PSS 1 | 0.8 | 2186 | 2.60 | - 1.5% |
| PSS 2 | 1 | 2263 | 2.65 | + 1.8% |

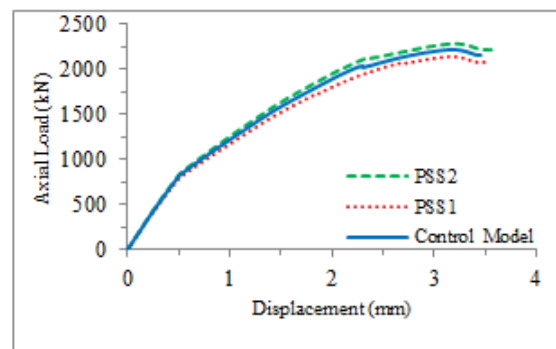


Fig 7. Axial load–displacement curves of the composite wall with varying PSS thicknesses

B. Embedded rectangular CFS without stiffener

To improve axial load resistance of the composite wall, three FE models were generated and analyzed by using embedded rectangular CFS with different thicknesses and without any stiffener. The models ER1, ER2, and ER3 represent the composite wall with an embedded rectangular CFS that is 0.8, 0.9, and 1.0 mm thick, respectively. TABLE V and Fig. 8 present the ultimate axial loads of 2767, 2941, and 2995 kN for models ER1, ER2, and ER3, which demonstrate an improvement of 24%, 32%, and 34% from the control model (2221 kN), respectively as shown in Fig. 7.

Given these improvements, this study suggests using an embedded rectangular CFS with a thickness of 0.9 mm for the composite wall system because it exhibits optimum behavior and higher economy than other thickness values.

TABLE V
AXIAL LOAD RESISTANCE OF THE COMPOSITE WALL THAT IS ATTRIBUTED TO THE THICKNESS OF THE RECTANGULAR CFS

| Models | Rectangular Strengthening Thickness (mm) | Axial Load (KN) | Displacement (mm) | Improvement Percentages |
|---------------|--|-----------------|-------------------|-------------------------|
| Control Model | - | 2221 | 3.1 | - |
| ER1 | 0.8 | 2767 | 2.8 | + 24% |
| ER2 | 0.9 | 2941 | 3.2 | + 32% |
| ER3 | 1.0 | 2995 | 3.0 | + 34% |

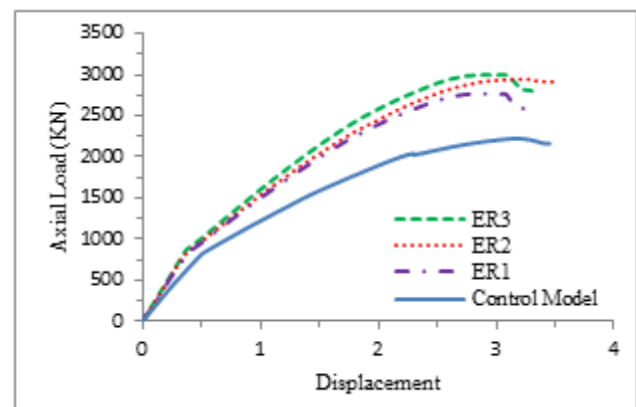


Fig 8. Axial load–displacement curves of the composite wall with embedded rectangular CFS to strengthen thickness

C. Embedded rectangular CFS with stiffeners

This study generated two FE composite walls models with

embedded rectangular CFS supported by L-and T-shaped stiffeners, named ER2-SL and ER2-ST, respectively. Each model was designed with a unique stiffener tied to each internal face of the embedded rectangle, as shown in Fig. 8. These FE models were compared with the control model to investigate the effectiveness of the stiffeners on the behavior of the composite wall against the axial load.

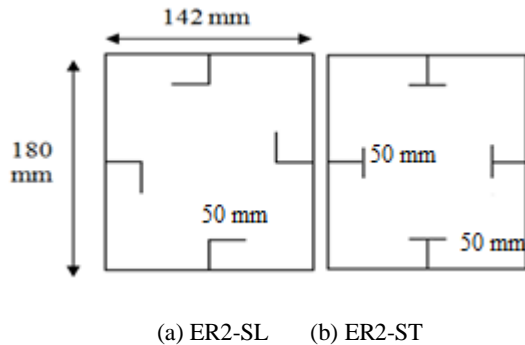


Fig 9. Embedded rectangular CFS with stiffeners

TABLE VI and Fig. 10 clearly show the increasing axial load resistance for the aforementioned FE models compared with the control model. Moreover, the improvement percentage was +54% for model ER2-SL, whereas model ER2-ST exhibited higher axial load resistance, that is, +62% more than the control model as shown in Fig. 9. This change was attributed to the T-shaped stiffener. Model ER2 exhibited an axial load resistance that is +32% higher than the control model with a maximum displacement equal to 3 mm, whereas the displacement of models ER2-SL and ER2-ST reached 7.0 mm. These results indicate that the ductility of the composite wall was improved compared with that of the control model.

TABLE VI
AXIAL LOAD RESISTANCE OF THE COMPOSITE WALL STRENGTHENED WITH RECTANGULAR CFS

| Models | Strengthening Shapes | Displacement (mm) | Axial load Resisting (KN) | Improvement Percentage |
|---------------|----------------------|-------------------|---------------------------|------------------------|
| Control Model | - | 3.0 | 2221 | 0 |
| ER2 | - | 3.2 | 2941 | + 32% |
| ER2-SL | L Shape | 7.0 | 3430 | + 54% |
| ER2-ST | T Shape | 7.0 | 3603 | + 62% |

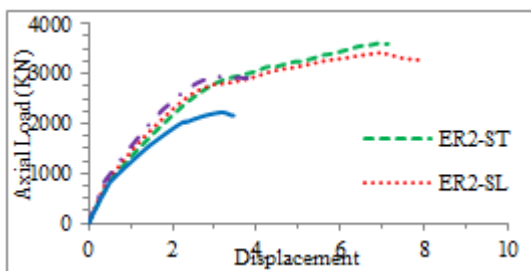


Fig 10. Axial load-displacement curves of the composite wall with embedded rectangular CFS supported by L-and T-shaped thickeners to strengthen thickness

VI. CONCLUSION

FE models were developed and presented in this study to verify the axial load behavior of an existing experimental

composite wall. Seven FE models were analyzed using Abaqus/CAE to create three different novel parameters to verify the axial load behavior of the composite wall by considering the effects of PSS thickness, embedded rectangular CFS thickness without stiffener, and embedded rectangular CFS with stiffeners. The variable information provided by the parametric study can be summarized as follows. First, the effect of PSS thickness on the axial load behavior of the composite wall was minimal, and the percentage difference between the control model and the composite walls with different PSS thicknesses was only +1.0%. Thus, this study suggests using PSS with 0.8 mm thickness. Second, the result of the comparisons between the FE composite wall models strengthened by embedded rectangular CFS with different thicknesses and the control model proved that the axial load behavior of the composite walls increased by different percentages more than the control model. Therefore, this study suggests using rectangular CFS that is 0.9 mm thick for strengthening. Third, the comparisons between the control model and the FE composite wall models strengthened by an embedded rectangular CFS supported by stiffeners with two different shapes proved that the stiffeners had a considerable positive effect with different percentages that were approximately +62% higher than the control model. Thus, this study suggests using rectangular CFS supported by T-shaped stiffener.

In summary, to increase axial load resistance and for economical purposes, the suggested composite wall should have a PSS that is 0.8 mm thick, an embedded rectangular CFS that is 0.9 mm thick, and a T-shaped stiffener to strengthen the rectangular CFS.

ACKNOWLEDGMENT

The authors acknowledge the study leave program of the University of Technology, Baghdad, Iraq and the financial support provided for the study.

REFERENCES

- [1] Wright, H. (1998). The axial load behaviour of composite walling. *Journal of Constructional Steel Research*, 45(3), 353-375 [http://dx.doi.org/10.1016/S0143-974X\(97\)00030-8](http://dx.doi.org/10.1016/S0143-974X(97)00030-8).
- [2] S. Rafiei, K. M. A. Hossain, M. Lachemi, K. Behdinan, and M. S. Anwar, "Finite element modeling of double skin profiled composite shear wall system under in-plane loadings," *Engineering Structures* vol. 56 pp. 46–57, 2013. <http://dx.doi.org/10.1016/j.engstruct.2013.04.014>
- [3] Hossain KMA and W. HD, "Experimental and theoretical behavior of composite walling under in-plane shear," *J Construct Steel Res* vol. 60, pp. 59–83, 2004. <http://dx.doi.org/10.1016/j.jcsr.2003.08.004>
- [4] H. KMA and W. HD, "Performance of double skin profiled composite shear walls—experiments and design equations," *Can J Civil Eng* vol. 31, pp. 204–17, 2004. <http://dx.doi.org/10.1139/103-087>
- [5] H. KMA and W. HD, "Performance of profiled concrete shear panels," *J Struct Eng, ASCE*, vol. 124, pp. 368–81, 1998. [http://dx.doi.org/10.1061/\(ASCE\)0733-9445\(1998\)124:4\(368\)](http://dx.doi.org/10.1061/(ASCE)0733-9445(1998)124:4(368))
- [6] R. S, H. KMA, L. M, and B. K, "Shear buckling of profiled steel sheets under in-plane monotonic loadings " presented at the CSCE 2nd international structures speciality conference, Winnipeg, Manitoba, 2010.
- [7] S. Hamzah and W. H. W. Badaruzzaman, "Structural Evaluation Of PSSDB Wall Panel With Square Opening And Varied Screw Spacing," *Journal of Engineering Science and Technology* vol. 4, pp. 32 – 46, 2009.

- [8] N. HanizamAwang, Wan Hamidon Wan Badaruzzaman, "Complete Application of Profiledd Steel Sheeteding Dry Board System as School Classroom Modules," presented at the 2nd International Conference On Built Environment In Developing Countries 2008.
- [9] M. Surat, W. H. W. Badaruzzaman, M. M. Tahir, and N. A. G. Abdullah, "Current Application of Pressed Steel Sheeted Dry Board (PSSDB) Modulation Panels for Annex Classroom Blocks in Melaka Malaysia," UNITEN ICCBT vol. B, pp. 433-452, 2008.
- [10] S. H., Y. C.B., and W. H. W. B., "Effect Of Butt Joint On PSSDB Wall Panel With Door Opening Under Axial Load," alaysian Construction Research Journal (MCRJ), vol. 1, 2007.
- [11] C. B. Yong, S. H. Hamzah, and W. H. Wan Badaruzzaman, "Structural behavior of profiledd steel sheeted dry board system wall panel with window opening.," presented at the 20th Conference of ASEAN Federation of Engineering Organization (CAFEO 20), Cambodia, 2002.
- [12] P. Prabha, V. Marimuthu, M. Saravanan, G. S. Palani, N. Lakshmanan, and R. Senthil, "Effect of confinement on steel-concrete composite light-weight load-bearing wall panels under compression," SciVerseScienceDirect, 24 November 2012.
- [13] P. Prabha, V. Marimuthu, M. Saravanan, G. S. Palani, N. Lakshmanan, and R. Senthil, "Effect of confinement on steel-concrete composite light-weight load-bearing wall panels under compression," Journal of Constructional Steel Research, vol. 81, pp. 11-19, 2/ 2013.
- [14] K M Anwar Hossain, "Axial load behaviour of pierced profiled composite walls," presented at the IPENZ Transactions, 2000.
- [15] K. KH, "Workability, testing, and performance of self-consolidating concrete," ACI Mater J, vol. 96, pp. 346-53, 1999.
- [16] S. a. M, L. M, H. KMA, R. R, and L. VC, "Influence of aggregate type and size on ductility and mechanical properties of engineered cementitious composites.," ACI Mater J, vol. 106, pp. 308-16, 2009.
- [17] L. J, O. J, O. S, and O. E, "A plastic-damage model for concrete," Int J Solids Struct vol. 25, pp. 299-326, 1989.
[http://dx.doi.org/10.1016/0020-7683\(89\)90050-4](http://dx.doi.org/10.1016/0020-7683(89)90050-4)

Salam Jasim Hilo. PhD student in the Department of Civil and Structural Engineering, Universiti Kebangsaan Malaysia (UKM), Bangi, Selangor, Malaysia since 2009 to date. BE in Civil Engineering from University of Technology, Baghdad, Iraq in 2007. MSc in Civil and Structural Engineering with an excellent grade from Universiti Kebangsaan Malaysia (UKM) in 2011. Two years of industrial experience in Civil Engineering. Assistant lecturer at University of Technology, Baghdad, Iraq. Research interests: steel and composite structural elements and their behavior and also engineering software for structural elements analysis.

Wan Hamidon WAN BADARUZZAMAN. Professor in the Department of Civil and Structural Engineering, Universiti Kebangsaan Malaysia (UKM), Bangi, Selangor, Malaysia. PhD in Structural Engineering from the University of Wales, Cardiff, UK in 1994. Twenty-six years of vast teaching, training, research, publication, administration, accreditation and consultancy experiences. On secondment, was the Chief Executive Officer of the UKM Perunding Kejuruteraan & Arkitek Sdn. Bhd., a university professional consultancy company. Research interests: steel_concrete composite structural elements, light weight, cold-formed composite structures and their behavior.

Siti Aminah OSMAN. Dr, Senior lecturer in the Department of Civil and Structural Engineering, Universiti Kebangsaan Malaysia (UKM), Bangi, Selangor, Malaysia. A member of Board of Engineers Malaysia (BEM). Graduated from Universiti Teknologi Malaysia in 1992 with BE (Hons), MSc in Structural Engineering from University of Bradford, UK in 1995 and PhD in Civil and Structural Engineering from Universiti Kebangsaan Malaysia (UKM) in 2006. After undergraduate studies, started teaching as a lecturer at Universiti Kebangsaan Malaysia (UKM). Research interests: structural engineering, wind engineering and industrial building system (IBS) construction.

Ahmed W. Al-Zand. PhD student in the Department of Civil and Structural Engineering, UniversitiKebangsaanMalaysia (UKM), Bangi, Selangor, Malaysia since 2013 to date. BE in Civil Engineering from University of Al-Mustansirya, Baghdad, Iraq in 1999. MSc in Civil and Structural Engineering with very good grade from Al-Mustansirya, Baghdad, Iraq in 2002. Fourteen years of site and design experience in structuralengineering fields. Senior structural engineers for several projects in Iraq, Oman, UAE & Qatar. Research interests: steel and composite structural members.